Integration of PMSG-Based Wind Turbine into Electric Power Distribution System Load Flow Analysis

RUDY GIANTO, MANAGAM RAJAGUKGUK
Department of Electrical Engineering, University of Tanjungpura, INDONESIA

Abstract: In this paper, a simple method for modeling and integrating PMSG (Permanent Magnet Synchronous Generator)-based WPP (Wind Power Plant) for load flow analysis of electric power distribution systems is proposed. The proposed model is derived based on: (i) the PMSG torque current equations, (ii) the relationships between PMSG voltages/currents in q-axis and d-axis, and (iii) the equations of WPP powers (namely: turbine mechanical power input, WPP power loss and power output). Application of the proposed model in representative electric power distribution system is also investigated and presented in this paper. The results of the investigation confirm the proposed model validity. The confirmation can also be verified by observing the load flow analysis results where, for each value of turbine power, the substation power output plus the WPP power output is always equal to the total system load plus total line loss (the line loss has been calculated based on the impedances and currents of the distribution lines).

Key-Words: PMSG, wind power plant, steady state model, load flow analysis, distribution system

Received: March 21, 2021. Revised: January 8, 2022. Accepted: February 18, 2022. Published: March 14, 2022.

1 Introduction

Based on the rotational speed, WPPs can be classified into two groups, namely: (i) fixed or near-constant speed WPP and (ii) variable speed WPP. Since variable-speed WPP can capture or extract wind energy in a more optimal way than fixed-speed WPP, its application is currently much more popular. Two types of generators that are often used in variable-speed WPP configurations are DFIG (Doubly Fed Induction Generator) and PMSG [1,2]. Compared to DFIG, PMSG has an advantage in that it does not require direct current (DC) excitation because the magnetic field is obtained from permanent magnets. Thus, PMSG does not require slip rings and brushes, which reduces power losses and simplifies maintenance. Furthermore, the PMSG-based WPP can operate at low speed, so it does not need a gearbox. Therefore, the construction can be made simpler, more robust, efficient, and the cost is also cheaper [1,2].

Load flow analysis provides information about the steady-state conditions of an electric power system. In load flow analysis, a conventional synchronous generator is generally expressed as a generator with constant active power and voltage magnitude (commonly known as the PV model). However, with the penetration of WPP, which usually does not use conventional synchronous generator, the PV model can no longer be used to represent the WPP, and consequently the load flow analysis cannot be carried out. Therefore, to enable of such analysis to be carried out, developing a valid model for the WPP and modifying the traditional load flow analysis is necessary. Several researchers have conducted studies on the modeling and integration of WPP in load flow analysis, and some of the recent methods are reported in [3-18].

References [3-11], propose some interesting methods to incorporate fixed-speed WPP into load flow analysis of multi-bus electric power system. On the other hand, researchers in [12-18] propose several DFIG-based variable speed WPP models to be used in load flow analysis of electric power systems. However, steady state modeling of PMSG-based WPP for load flow analysis has not been much investigated and reported in the literatures.

This paper proposes a simple method for modeling and integrating PMSG-based variable speed WPP in the electric power distribution system load flow analysis. The proposed model is derived based on (i) the PMSG torque current equations, (ii) the relationships between PMSG voltages/currents in q-axis and d-axis, and (iii) the WPP powers (namely: turbine mechanical power input, WPP power loss, and power output).

Furthermore, this paper also discusses a case study where validation of the proposed method is carried out.

2 Formulation of DSLF Problem

As previously mentioned, load flow study is normally carried out to evaluate the steady-state performance of an electric power system. The electrical quantities such as bus voltages, power generations, transmission/distribution line power flows (and losses) can be determined from the study. It can be shown that the load flow problem of an electric power distribution system has the following formulations [19-21]:

$$P_{Gi} - P_{Li} - \sum_{j=1}^{n} |V_i||Y_{ij}||V_j| cos(\delta_i - \delta_j - \theta_{ij}) = 0 \quad (1a)$$

$$Q_{Gi} - Q_{Li} - \sum_{j=1}^{n} |V_i||Y_{ij}||V_j| sin(\delta_i - \delta_j - \theta_{ij}) = 0 \quad (1b)$$

By observing (1), it can be seen that for each system bus, there will be two equations and four unknown quantities (i.e. P_G, Q_G, $|V|$ and δ). Therefore, in order to find a unique solution to (1), two of the four quantities values must be determined or specified. For this purpose, it is a common practice in distribution load flow analysis to define two types of buses, namely: (1) substation bus (reference); and (2) load bus (see Table 1).

Table 1. Known and unknown quantities

Bus	Known Quantities	Unknown Quantities
SS*	$\|V\|$ and $\delta=0$	P_G and Q_G
Load	$P_G=Q_G=0$	$\|V\|$ and δ

*SS: Substation

3 PMSG-Based Wind Turbine

3.1 Basic Structure

Figure 1 shows a basic configuration of PMSG-based WPP [1,2,22]. Power electronic devices (such as converter, inverter, and DC link) connect the PMSG to the electric power system (or power grid). With these power electronic devices, the PMSG rotation speed can be isolated from the frequency of the power system where the WPP is connected. This isolation makes the PMSG-based WPP can be operated at a broader generator speed range than other WPP types. Therefore, the wind energy extraction can be carried out more optimally. It is to be noted that in PMSG-based wind turbine, the power converter based on IGBT (Insulated Gate Bipolar Transistor) is usually employed for the power electronic device topology.

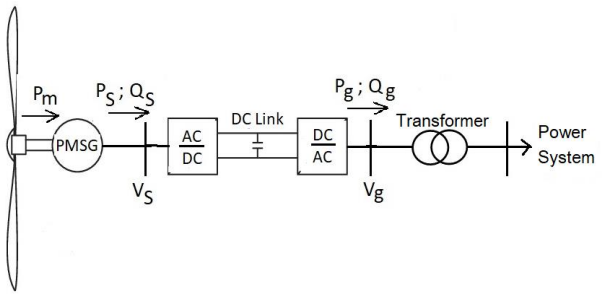

Fig. 1: PMSG-based wind turbine structure

In Figure 1, P_m is wind turbine mechanical power input; V_S is PMSG stator voltage; V_g is WPP terminal voltage; P_S and Q_S are PMSG active and reactive power outputs (powers at PMSG stator); P_g and Q_g are WPP active and reactive power outputs. It should also be noted that PMSG-based WPP has the ability to deliver or absorb reactive power (leading or lagging power factor operation) However, the unity power factor mode of operation is more often adopted. In this mode of operation, the WPP does not deliver or absorb reactive power to or from the power grid.

3.2 PMSG Equivalent Circuits

Figure 2 shows the PMSG equivalent circuits in d-q reference frame [22-26]. In the figure, V_q and V_d are q- and d-axis terminal voltages; I_q and I_d are q- and d- axis terminal currents; I_{wq} and I_{wd} are q- and d-axis torque currents; R_S is stator winding resistance; L_q and L_d are PMSG inductances in q- and d-axis; ω_r is rotor angular speed; and Ψ_f is permanent magnet flux. It is to be noted that in Figure 2, R_{fe} and R_S are used to represent PMSG iron and copper losses, respectively. Copper loss occurs in the PMSG stator winding, while iron loss occurs in the PMSG iron core. Also, in Figure 2, I_{feq} and I_{fed} quantities are used to express the currents flowing in R_{fe} in q- and d-axis, respectively.

Based on Figure 2, the PMSG terminal voltages will have the following forms:

$$V_q = \omega_r(\Psi_f - L_d I_{wd}) - R_S I_q \quad (2a)$$

$$V_d = \omega_r L_q I_{wq} - R_S I_d \quad (2b)$$

On the other hand, the PMSG torque currents can be formulated as:

$$I_{wq} = I_q + I_{feq} = I_q + \frac{\omega_r \left(\Psi_f - L_d I_{wd}\right)}{R_{fe}} \quad (3a)$$

$$I_{wd} = I_d + I_{fed} = I_d + \frac{\omega_r L_q I_{wq}}{R_{fe}} \quad (3b)$$

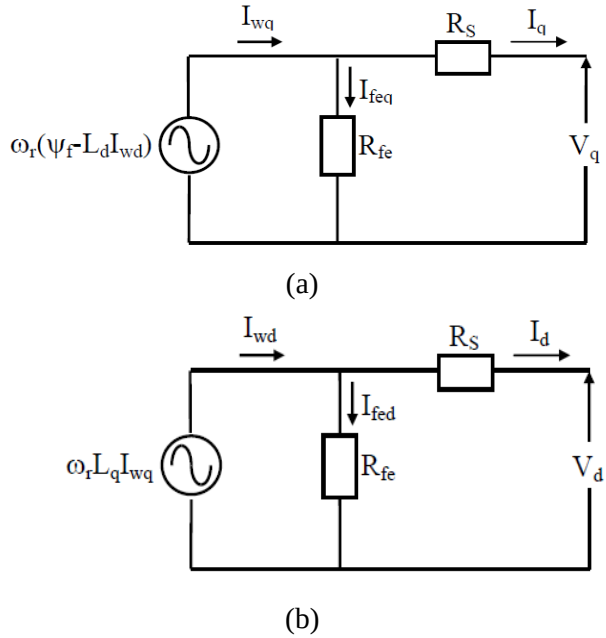

Fig. 2: PMSG equivalent circuits

The relationships between q- and d-axis quantities of the PMSG terminal voltage and current can be expressed as (see Figure 7 in Appendix A.1):

$$V_d = V_q \tan\beta \quad (4a)$$

$$I_d = I_q \tan\beta \quad (4b)$$

where β is the angle of PMSG rotor relative to the stator voltage/current.

3.3 PMSG Power Formulations

By looking at Figure 1, it can be seen that the PMSG power output equals to turbine mechanical power input minus PMSG copper loss (P_{cu}) and PMSG iron loss (P_{fe}), or:

$$P_S = P_m - P_{cu} - P_{fe} \quad (5)$$

It should be noted that in (5) the mechanical or friction loss due to rotation of the PMSG rotor have been neglected because their value is much smaller than the other losses [23,24]. On the other hand, the PMSG power output can also be formulated as a function of the stator voltage and current as follows (derivation can be found in Appendix A.1):

$$P_S = 0.5\left(V_q I_q + V_d I_d\right) \quad (6)$$

Also, the PMSG copper loss (P_{cu}) and PMSG iron loss (P_{fe}) in (5) can be calculated using the following formulas [23,24]:

$$P_{cu} = 0.5 R_s \left(I_q^2 + I_d^2\right) \quad (7)$$

$$P_{fe} = 0.5 R_{fe} \left(I_{feq}^2 + I_{fed}^2\right) \quad (8)$$

Therefore, on using (6) - (8) in (5), the turbine power can be formulated as:

$$P_m = 0.5\left(V_q I_q + V_d I_d\right) + 0.5 R_s \left(I_q^2 + I_d^2\right) + 0.5 R_{fe} \left(I_{feq}^2 + I_{fed}^2\right) \quad (9)$$

3.4 PMSG Modeling and Integration

Based on (3), (4) and (9), the proposed steady state model of PMSG-based WPP is:

$$R_{fe}\left(I_{wq} - I_q\right) - \omega_r \left(\Psi_f - L_d I_{wd}\right) = 0 \quad (10a)$$

$$R_{fe}\left(I_{wd} - I_d\right) - \omega_r L_q I_{wq} = 0 \quad (10b)$$

$$V_d - V_q \tan\beta = 0 \quad (10c)$$

$$I_d - I_q \tan\beta = 0 \quad (10d)$$

$$P_m - 0.5\left(V_q I_q + V_d I_d\right) - 0.5 R_s \left(I_q^2 + I_d^2\right) - 0.5 R_{fe} \left(I_{feq}^2 + I_{fed}^2\right) = 0 \quad (10e)$$

In (10a) and (10b), the torque currents (I_{wq} and I_{wd}) are calculated based on (2) as follows:

$$I_{wq} = \left(V_d + R_s I_d\right) / \omega_r L_q \quad (11a)$$

$$I_{wd} = \left(\omega_r \Psi_f - R_s I_q - V_q\right) / \omega_r L_d \quad (11b)$$

It can be seen from (11) that the PMSG torque currents have been represented in terms of PMSG terminal voltage and current. Based on Figure 2, I_{feq} and I_{fed} in (10e) can also be expressed in terms of PMSG terminal voltage and current as follows:

$$I_{feq} = I_{wq} - I_q = \frac{V_d + R_s I_d}{\omega_r L_q} - I_q \qquad (12a)$$

$$I_{fed} = I_{wd} - I_d = \frac{\omega_r \Psi_f - R_s I_q - V_q}{\omega_r L_d} - I_d \qquad (12b)$$

Therefore, for electric power system embedded with PMSG-based WPP, solution to the load flow problem is found by simultaneously solving the nonlinear equations (1) and (10). Table 2 shows the known (specified) and unknown (to be calculated) quantities in the equations. It should be noted that, in the load flow analysis, the following relationships also apply:

$$P_G = P_g = \eta_{PEC} P_S = 0{,}5 \eta_{PEC} \left(V_q I_q + V_d I_d \right) \qquad (13a)$$

$$Q_G = Q_g = \eta_{PEC} Q_S = 0 \qquad (13b)$$

where η_{PEC} is efficiency of the power electronic converter. In (13b), the WPP reactive power output is zero because the PMSG-based WPP is assumed to be operated at unity power factor or no reactive power exchange between the WPP and the power grid. It is also to be noted that since set of equations (1) and (10) is nonlinear, iterative techniques (for example Newton-Raphson method) are often employed to solve the set of equations. Brief explanation of Newton-Raphson method is given in Appendix A.2.

Table 2. Known and unknown quantities for system with WPP

Bus	Known Quantities	Unknown Quantities
SS	$\|V\|$ and $\delta=0$	P_G and Q_G
Load	$P_G=Q_G=0$	$\|V\|$ and δ
WPP	ω_r, P_m, R_S, R_{fe}, L_d, L_q, Ψ_f, and η_{PEC}	$\|V=\|V_g\|$, $\delta=\delta_g$, V_q, V_d, I_q, I_d and β

4 Case Study

4.1 Test System

Distribution system shown in Figure 3 will be used in the case study to investigate the application of the proposed model in load flow analysis of electric power distribution system containing PMSG-based WPP. The system in Figure 3 has 33 buses and is adopted from [19,20]. The system has a voltage of 12.66 kV with a total three-phase load of 11.145 MW and 6.900 MVAR. The system is then modified by adding a PMSG-based WPP in the system. The WPP is connected to bus 33 via a step-up transformer. All of the system data (including WPP data) are shown in Tables 3 and 4. Unless otherwise stated, all data are in pu on the basis of 1 MVA.

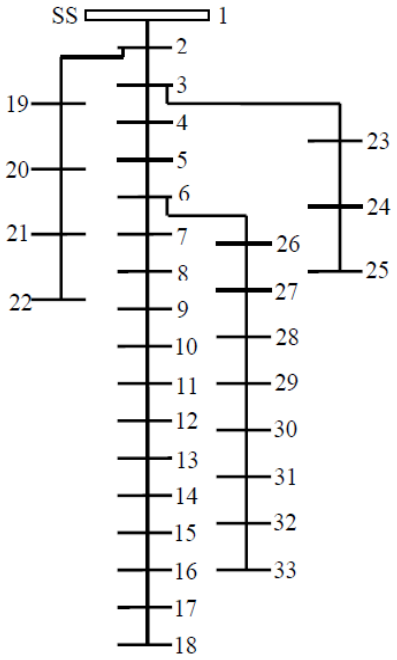

Fig. 3: Test system

Table 3. Test system data

Br. No	Send Bus	Rec. Bus	R (pu)	X (pu)	P_L* (pu)	Q_L* (pu)
1	1	2	0.000575	0.000293	100	60
2	2	3	0.003076	0.001567	90	40
3	3	4	0.002284	0.001163	120	80
4	4	5	0.002378	0.001211	60	30
5	5	6	0.005110	0.004411	60	20
6	6	7	0.001168	0.003861	200	100
7	7	8	0.010678	0.007706	200	100
8	8	9	0.006426	0.004617	60	20
9	9	10	0.006514	0.004617	60	20
10	10	11	0.001227	0.000406	45	30
11	11	12	0.002336	0.000772	60	35
12	12	13	0.009159	0.007206	60	35
13	13	14	0.003379	0.004448	120	80

14	14	15	0.003687	0.003282	60	10
15	15	16	0.004656	0.003400	60	20
16	16	17	0.008042	0.010738	60	20
17	17	18	0.004567	0.003581	90	40
18	2	19	0.001023	0.000976	90	40
19	19	20	0.009385	0.008457	90	40
20	20	21	0.002555	0.002985	90	40
21	21	22	0.004423	0.005848	90	40
22	3	23	0.002815	0.001924	90	50
23	23	24	0.005603	0.004424	420	200
24	24	25	0.005590	0.004374	420	200
25	6	26	0.001267	0.000645	60	25
26	26	27	0.001773	0.000903	60	25
27	27	28	0.006607	0.005826	60	20
28	28	29	0.005018	0.004371	120	70
29	29	30	0.003166	0.001613	200	600
30	30	31	0.006080	0.006008	150	70
31	31	32	0.001937	0.002258	210	100
32	32	33	0.002128	0.003308	60	40

*Load connected to receiving bus

Table 4. Wind turbine generator data

Turbine	Length of turbine blade: 38 meter Power rating: 2.0 MW Speed: Cut-in: 3 m/s; Rated: 14 m/s; Cut-out: 23 m/s
Gearbox	None (Direct drive)
Generator	Type: PMSG Power rating: 2.0 MW Number of pole pairs: 26 Voltage: 690 Volt Speed rating: 22.5 rpm Resistance/Induktance/Flux: R_S=0.02; R_{fe}=80; L_d=2.0; L_q=3.0; Ψ_f =2.3
Power electronic converter	Efficiency: η_{PEC} = 95%
Transformer	Impedance: j0.1 Ohm

4.2 Calculation of Wind Power

Turbine mechanical power and rotor speed can be calculated using the formulas given [15]. In the calculation it is assumed that the air density is 1.225 kg/m^3, tip speed ratio is 7.0, and turbine performance coefficient is 0.4. Table 5 shows the calculation results of turbine mechanical power and rotor speed for wind speed values ranging from 5 to 12 m/s.

Table 5. Turbine power and rotor speed

V_w (m/s)	ω_r (rad/s)	P_m (MW)
5	23.9474	0.1389
6	28.7368	0.2401
7	33.5263	0.3812
8	38.3153	0.5691
9	43.1053	0.8102
10	47.8947	1.1114
11	52.6842	1.4793
12	57.4737	1.9206

4.3 Results and Discussion

Tables 6 and 7 show the load flow analysis results for various values of turbine mechanical power as listed in Table 5. Some of the results are also presented in graphical forms (see Figures 4 - 6). It can be seen that as the turbine mechanical power increases, PMSG power losses also increase. The increase in power losses is due to the increase in PMSG power output which can be explained as follows. As the PMSG power output raises, the generator currents and losses will also increase.

Due to power loss in the power electronic converter, the power output of WPP (P_g) is slightly smaller than PMSG stator power (P_S) (see Figure 4). In this paper, it has been assumed that the power converter has the efficiency of 95%. It is also to be noted that the WPP power output and the PMSG stator power vary linearly with the increase in turbine mechanical power.

Table 6. PMSG losses and WPP output

P_m (MW)	P_{cu} (MW)	P_{fe} (MW)	P_S (MW)	P_g (MW)
0,1389	0.0003	0.0151	0.1236	0.1174
0,2401	0.0006	0.0215	0.2180	0.2071
0,3812	0.0014	0.0379	0.3419	0.3248
0,5691	0.0024	0.0401	0.5266	0.5003
0,8102	0.0032	0.0456	0.7614	0.7234
1,1114	0.0052	0.0534	1.0528	1.0001
1,4793	0.0085	0.0587	1.4120	1.3414
1,9206	0.0118	0.0605	1.8483	1.7559

Table 7. WPP voltage, SS output and line loss

P_m (MW)	V_g (pu)	SS Power (MW, MVAR)	Line Loss (MW, MVAR)
0,1389	0.9836	11.5683+j7.2663	0.5406+j0.3663
0,2401	0.9849	11.4692+j7.2599	0.5313+j0.3599
0,3812	0.9866	11.3396+j7.2519	0.5194+j0.3519
0,5691	0.9892	11.1444+j7.2405	0.4997+j0.3405
0,8102	0.9924	10.9045+j7.2276	0.4828+j0.3276
1,1114	0.9963	10.6053+j7.2132	0.4605+j0.3132
1,4793	1.0012	10.2399+j7.1981	0.4362+j0.2981
1,9206	1.0070	9.7908+j7.1833	0.4017+j0.2833

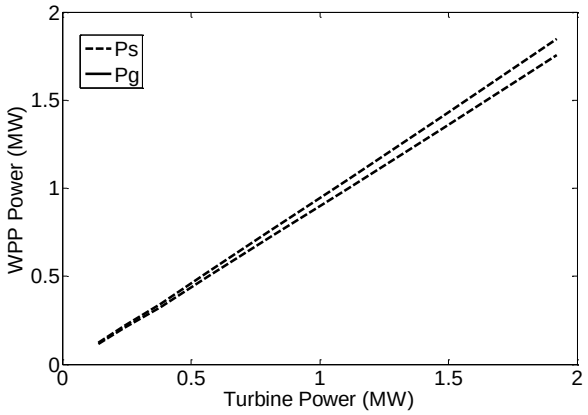

Fig. 4: Variation of WPP power

The load flow study results also show that with the increase in WPP power output, the voltage profile will also improve (see Figure 5). This voltage profile improvement can occur because with the increase in WPP power output, more loads can be supplied by the WPP, and the line losses will be decreasing since the WPP is located at the end of the distribution line. In turn, this line losses decrement reduces the line voltage drop and improves the system voltage profile.

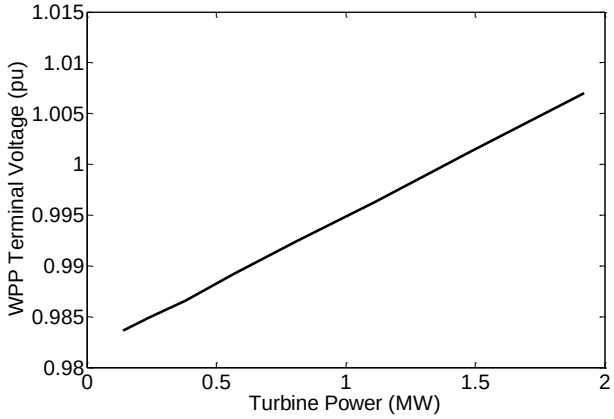

Fig. 5: Variation of WPP voltage

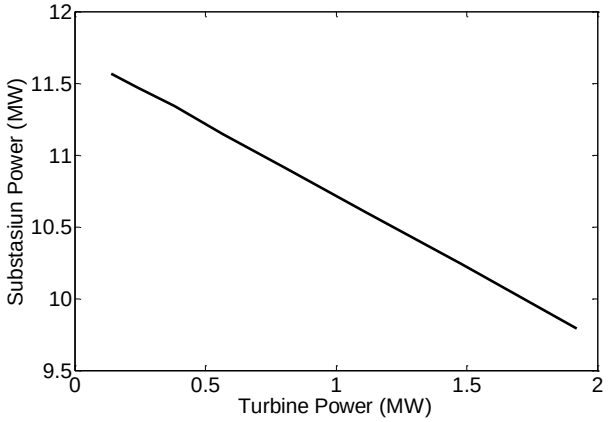

Fig. 6: Variation of substation power

Beside the system voltage profile improvement, another advantage of the WPP installation is that it can reduce the power supply from distribution system substation (see Figure 6). It is to be noted that power supply from distribution substation usually comes from conventional power plants that use non-renewable energy sources. It is to be noted the results of the above study also confirm the proposed method validity. More confirmation can also be obtained by observing the results of load flow analysis where, for each value of turbine power, the substation power output plus the WPP power output is always equal to the total system load plus total line loss. Where the line loss has been calculated based on the impedances and currents of the distribution lines.

5 Conclusion

In this paper, a simple method for modeling and integrating PMSG-based variable speed WPP for load flow analysis of electric power distribution systems has been proposed. The proposed model is derived based on: (i) the PMSG torque current equations, (ii) the relationships between PMSG voltages/currents in q-axis and d-axis, and (iii) the equations of WPP powers (namely: turbine mechanical power input, WPP power loss and power output). Application of the proposed model in load flow analysis of representative electric power distribution system has also been investigated and presented in this paper. The results of the investigation (i.e., the load flow analysis results for various values of turbine mechanical power) confirm the proposed model validity.

The confirmation can also be obtained by observing the results of load flow analysis where, for each value of turbine power, the substation power output plus the WPP power output is always equal to the total system load plus total line loss, where the line loss has been calculated based on the impedances and currents of the distribution lines. However, in this paper, the PMSG-based WPP has been assumed to be operated at unity power factor. Extension of the method so that it can be applied to PMSG operating at lagging and leading power factors is probably an interesting topic for future research.

Appendix

A.1 PMSG Power Output

Figure 7 shows phasor diagrams of PMSG stator voltage and current [21,22]. In the figure, β is the

angle of PMSG rotor relative to the stator voltage/current. At steady state condition, this angle is constant. On the other hand, α is the angle of stator voltage/current to the reference. It is to be noted that V_S and I_S are in phase because the PMSG is operated at unity power factor ($Q_S=0$). Based on Figure 7, the formulas for stator voltage and current phasors are:

$$\overline{V_S} = \frac{1}{\sqrt{2}}\left(V_q - jV_d\right)e^{j(\beta+\alpha)} \quad \text{(A.1)}$$

$$\overline{I_S} = \frac{1}{\sqrt{2}}\left(I_q - jI_d\right)e^{j(\beta+\alpha)} \quad \text{(A.2)}$$

PMSG stator power can be calculated using:

$$\overline{S_S} = \overline{V_S}\,\overline{I_S}^{*} \quad \text{(A.3)}$$

Substituting (A.1) and (A.2) into (A.3), the PMSG stator power becomes:

$$\overline{S_S} = 0{,}5\left[\left(V_q I_q + V_d I_d\right) + j\left(V_q I_d - V_d I_q\right)\right] \quad \text{(A.4)}$$

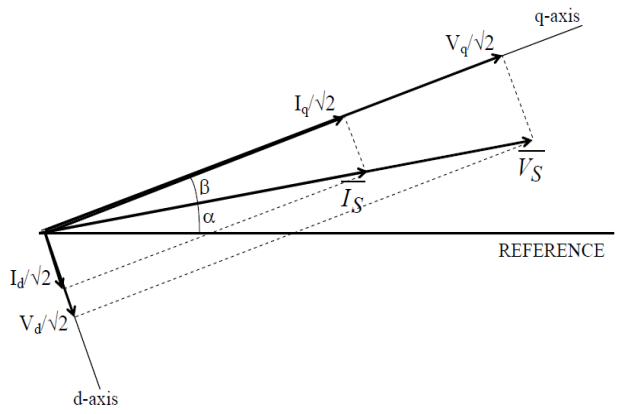

Fig. 7: Phasor diagrams of stator voltage and current of PMSG

By separating the real and imaginary parts of (A.4), the formulas for PMSG stator active and reactive powers are:

$$P_S = Re\left(\overline{S_S}\right) = 0{,}5\left(V_q I_q + V_d I_d\right) \quad \text{(A.5)}$$

$$Q_S = Im\left(\overline{S_S}\right) = 0{,}5\left(V_q I_d - V_d I_q\right) = 0 \quad \text{(A.6)}$$

A.2 Newton-Raphson Method

In general form, a set of nonlinear equations can be written as:

$$\boldsymbol{F}(\boldsymbol{x}) = \begin{bmatrix} f_1(x_1, x_2, \ldots, x_n) \\ f_2(x_1, x_2, \ldots, x_n) \\ \vdots \\ f_n(x_1, x_2, \ldots, x_n) \end{bmatrix} = \boldsymbol{0} \quad \text{(A.7)}$$

In Newton-Raphson method, the calculation of unknown variables x_i, is conducted by solving:

$$\boldsymbol{x}^{(k+1)} = \boldsymbol{x}^{(k)} + \boldsymbol{d}^{(k)} \quad \text{(A.8)}$$

where:

$$\boldsymbol{d}^{(k)} = -\left[\boldsymbol{J}(\boldsymbol{x}^{(k)})\right]^{-1}\boldsymbol{F}(\boldsymbol{x}^{(k)}) \quad \text{(A.9)}$$

In (A.9), $\boldsymbol{J}(\boldsymbol{x})$ is the Jacobian of $\boldsymbol{F}(\boldsymbol{x})$, and is determined using:

$$\boldsymbol{J}(\boldsymbol{x}) = \begin{bmatrix} \frac{\partial f_1}{\partial x_1} & \frac{\partial f_1}{\partial x_2} & \cdots & \frac{\partial f_1}{\partial x_n} \\ \frac{\partial f_2}{\partial x_1} & \frac{\partial f_2}{\partial x_2} & \cdots & \frac{\partial f_2}{\partial x_n} \\ \vdots & \vdots & \ddots & \vdots \\ \frac{\partial f_n}{\partial x_1} & \frac{\partial f_n}{\partial x_2} & \cdots & \frac{\partial f_n}{\partial x_n} \end{bmatrix} \quad \text{(A.10)}$$

References:

[1] Babu, N.R., and Arulmozhivarman, P.: 'Wind Energy Conversion System – A Technical Review', *Journal of Engineering Science and Technology*, 2013, Vol. 8, No. 4, pp. 493-507.

[2] Samraj, D.B., and Perumal, M.P.: 'Compatibility of Electrical Generators for Harvesting Extended Power from Wind Energy Conversion System', *Measurement and Control*, 2019, Vol. 52, No. 9-10, pp. 1-12.

[3] Haque, M.H.: 'Evaluation of Power Flow Solutions with Fixed Speed Wind Turbine Generating Systems', *Energy Conversion and Management*, 2014, Vol. 79, pp. 511-518.

[4] Haque, M.H.: 'Incorporation of Fixed Speed Wind Turbine Generators in Load Flow Analysis of Distribution Systems', *International Journal of Renewable Energy Technology*, 2015, Vol. 6, No. 4, pp. 317-324.

[5] Wang, J., Huang, C., and Zobaa, A.F., 'Multiple-Node Models of Asynchronous Wind Turbines in Wind Farms for Load Flow Analysis', *Electric Power Components and Systems*, 2015, Vol. 44, No. 2, pp. 135-141.

[6] Feijoo, A., and Villanueva, D.: 'A PQ Model for Asynchronous Machines Based on Rotor Voltage Calculation', *IEEE Trans. Energy Conversion*, 2016, Vol. 31, No. 2, pp. 813-814.

[7] Feijoo, A., and Villanueva, D.: 'Correction to 'A PQ Model for Asynchronous Machines Based on Rotor Voltage Calculation'', *IEEE Trans. Energy Conversion*, 2016, Vol. 31, No. 3, pp. 1228-1228.

[8] Gianto, R., Khwee, K.H., Priyatman, H., and Rajagukguk, M.: 'Two-Port Network Model of Fixed-Speed Wind Turbine Generator for Distribution System Load Flow Analysis', *TELKOMNIKA*, 2019, Vol. 17, No. 3, pp. 1569-1575.

[9] Gianto, R.: 'T-Circuit Model of Asynchronous Wind Turbine for Distribution System Load Flow Analysis', *International Energy Journal*, 2019, Vol. 19, No. 2, pp. 77-88.

[10] Gianto, R.: 'Steady state model of wind power plant for load flow study', in *Proceedings 2020 International Seminar on Intelligent Technology and Its Applications*, 2020, pp. 119-122.

[11] Gianto, R., and Khwee, K.H.: 'A New T-Circuit Model of Wind Turbine Generator for Power System Steady State Studies', *Bulletin of Electrical Engineering and Informatics*, 2021, Vol. 10, No. 2, pp. 550-558.

[12] Kumar, V.S.S., and Thukaram, D.: 'Accurate Modelling of Doubly Fed Induction Based Wind Farms in Load Flow Analysis', *Electric Power Systems Research*, 2018, Vol. 15, pp. 363-371.

[13] Ju, Y., Ge, F., Wu, W., Lin, Y., and Wang, J.: 'Three-Phase Steady-State Model of DFIG Considering Various Rotor Speeds', *IEEE Access*, 2016, Vol. 4, pp. 9479-948.

[14] Anirudh, C.V.S, and Seshadri, S.K.V.: 'Enhanced Modeling of Doubly Fed Induction Generator in Load Flow Analysis of Distribution Systems', *IET Renewable Power Generation*, 2021, Vol. 15, No. 5, pp. 980-989.

[15] Gianto, R.: 'Steady State Model of DFIG-Based Wind Power Plant for Load Flow Analysis', *IET Renewable Power Generation*, 2021, Vol. 15, No. 8, pp. 1724-1735.

[16] Gianto, R.: 'Integration of DFIG-Based Variable Speed Wind Turbine into Load Flow Analysis', in *Proceedings 2021 International Seminar on Intelligent Technology and Its Applications*, 2021, pp. 63-66.

[17] Gianto, R.: 'Steady State Load Flow of DFIG-Based Wind Turbine in Voltage Control Mode', in *Proceedings 2021 3rd International Conference on High Voltage Engineering and Power Systems*, 2021, pp. 232-235.

[18] Gianto, R.: 'Constant Voltage Model of DFIG-Based Variable Speed Wind Turbine for Load Flow Analysis', *Energies*, 2021, Vol. 14, No. 24, pp. 1-19.

[19] Gianto, R., and Khwee, K.H.: 'A New Method for Load Flow Solution of Electric Power Distribution System', *International Review of Electrical Engineering*, 2016, Vol. 11, No. 5, pp. 535-541.

[20] Gianto, R.: 'Application of Trust-Region Method in Load Flow Solution of Distribution Network Embedded with DREG', *International Review of Electrical Engineering*, 2021, Vol. 16, No. 5, pp. 418-427.

[21] Gianto, R., and Purwoharjono: 'Trust-Region Method for Load Flow Solution of Three-Phase Unbalanced Electric Power Distribution System', *Journal of Computer and Electrical Engineering*, 2022, Vol. 2022, pp. 1-17.

[22] Jain, A., Shankar, S., and Vanitha, V.: 'Power Generation Using PMSG Based Variable Speed Wind Energy Conversion System: An Overview', *Journal of Green Engineering*, 2018, Vol. 17, No. 4, pp. 477-504.

[23] Urusaki, N., Senjyu, T., and Uezato, K.: 'A Novel Calculation Method for Iron Loss Resistance Suitable in Modeling Permanent-Magnet Synchronous Motors', *IEEE Transactions on Energy Conversion*, 2003, Vol. 18, No. 1, pp. 41-47.

[24] Cavallaro, C., et al.: 'Efficiency Enhancement of Permanent-Magnet Synchronous Motor Drives by Online Minimization Approaches', *IEEE Transactions on Industrial Electronics*, 2005, Vol. 52, No. 4, pp. 1153-1160.

[25] Krause, P., and Wasynczuk, O.: *Analysis of Electric Machinary and Drive Systems*, 2013, Hoboken, NJ, USA: John Wiley & Sons. Inc.

[26] Boldea, I.: *Variable Speed Generators*, 2005, Roca Baton, FL, USA: Taylor & Francis Group LLC.